Water cooling of high power light emitting diode

Sørensen, Henrik

Published in:
Proceedings of the 13th IEEE Intersociety Conference on Thermal and Thermomechanical Phenomena in Electronic Systems (ITherm)

DOI (link to publication from Publisher):
10.1109/ITHERM.2012.6231531

Publication date:
2012

Document Version
Early version, also known as pre-print

Water Cooling of High Power Light Emitting Diode

Henrik Sørensen
Department of Energy Technology
Aalborg University
Pontoppidanstræde 101
Aalborg, Denmark, DK-9220
Phone: (+45) 2757 5280
Fax: (+45) 9815 1411
Email: hs@et.aau.dk

ABSTRACT

The development in light technologies for entertainment is moving towards LED based solutions. This progress is not without problems, when more than a single LED is used. The amount of generated heat is often in the same order as in a conventional discharge lamp, but the allowable operating temperature is much lower. In order to handle the higher specific power (W/m^3) inside the LED based lamps cold plates were designed and manufactured.

6 different designs were analyzed through laboratory experiments and their performances were compared. 5 designs cover; traditional straight mini channel, S-shaped mini channel, straight mini channel with swirl, threaded mini channel with swirl and 2 parallel mini channels with swirl. In the 6th design traditional mini channels were used. Based on the experimentally obtained heat transfer inside the cold plates, it was concluded that the mini channels utilizing swirling flow were much more efficient than channels with traditional flow without swirl. Similar conclusion was made for the design utilizing mini channels. Considering the pressure difference across the cold plate in addition to heat transfer properties, it turned out that two solutions were preferable; axial flow through mini channels or a s-channel. Experiments showed that the channel design utilizing swirling flows had up to 4 times the pressure loss as the mini channel/s-channel.

KEY WORDS: Heat transfer, Cooling, Cold plate, LED, Swirling flow, tangential inlets, mini channels.

NOMENCLATURE

A_c	cross sectional area, m^2
A_s	surfacel area, m^2
c_p	specific heat at constant pressure, $J/Kg\ K$
D	diameter, m
D_H	hydraulic diameter, m
f	friction factor, -
h	heat transfer coefficient, W/m^2K
h_∞	heat transfer coeff. (full developed flow), W/m^2K
k	thermal conductivity, $W/m\ K$
L	length, m
M_T	total momentum of axial flow, $kg\ m/s$
M_t	total momentum of tangential flow, $kg\ m/s$
$\dot{m}$	mass flow, kg/s
N	number of cooling channels, -
Nu	Nusselt number, -
Nu_s^*	norm. Nusselt number for swirl flow, -
Nu_{fd}^*	norm. Nusselt number for fully developed flow, -
Pr	Prandtl number, -
P	power, W
R	Thermal resistance, K/W
Re	Reynolds number, -
T	temperature, K
U	overall heat transfer coefficient, W/K
z_j	axial distance from inlet, m

Subscripts

a	air
b-hs	base to heat sink
C	cold plate
hs-w	heat sink to water
j	junction
j-b	junction to base
j-hs	junction to heat sink
j-ref	junction to reference thermistor
j-w	junction to water
ref-hs	reference thermistor to heat sink
ref-w	reference thermistor to water
w	water

INTRODUCTION

The recent years development of more compact electronically components has resulted in an increasing volume flux of heat, which becomes comparable in magnitude with e.g. a nuclear reactions [1]. The high rate of heat generated in the components result in a risk of having high operational temperatures, which causes problems with reliability and product lifetime.

The high power Light Emitting Diodes (LED) belongs to the group of electronics with increasing volume heat flux. The high power LEDs is becoming popular in the lighting industries, where it is considered as the "green" replacement of discharge light bulbs. The automotive industry has adopted the high power LEDs for front and rear light on cars and in near future this expands to include the forward head light. High power LEDs has problems with low efficiency, and together with a high current this leads to a heating problem. The heating problem is related to packaging design and this challenge is handled by the solid state lighting manufactures [2]. According to the magazine LED-professional [3] [4] continuous innovation on thermal management must take place - if the innovation shall continue inside LED light technologies. To address the thermal problem of the LEDs,

several researchers have conducted relevant studies on cooling solutions for the LEDs. The studies include discrete models for the temperature distribution of integrated LED light sources [5], microjet based cooling system for LED arrays [6], phase change heat sinks for high power LEDs [7], optimum design of radial heat sink on a LED [8] and thermal effects in packaging of high power LED arrays [9].

DESIGN OF COOLING SYSTEM FOR LED

A proper design for cooling of high power electronics depend on usage. For non-moving applications such as laptop computers, power converters etc. heat pipes seem to be an excellent heat mover, which makes it possible to move heat from a source inside a highly packed volume to areas with room for traditional heat sinks. In the case of external forces due to motion/acceleration, the heat pipe may stop working as the capillary forces are to weak to bring fluid back to the heat pipe evaporator side. For those type of applications a simple fluid cooling system driven by a mini pump may be the best solution. This kind of system is well known as cooler for extreme gaming computers, where both CPU and GPU are kept cold by small cold plates connected to a pump and traditional radiator (see figure 1). The same principle is used by Danfoss in their Shower Power cooling of high power Electronics. The analysis in this paper addresses design of a simple cold plate for cooling of a standard high power LED.

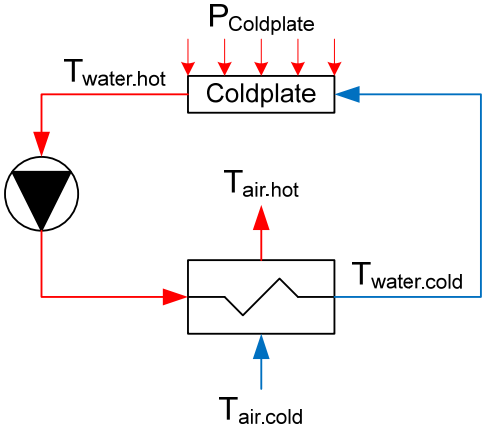

Figure 1: *Schematic view of cooling circuit for cooling of electronic components.*

The heat generated in the LED has to be removed in order to prevent failure and damage of the LED. The maximum LED junction temperature is dependent on fabricate and model. The blue Luminus CBT90 diode, which is used as example in this study, has a maximum allowable junction temperature of 150°C. This ensures a median life time of approximately 15000hours. The life time increases exponentially with temperature in cases where the junction temperature is below 150°C. With that in mind development engineers seek solutions, where as much heat as possible is transported away from the LED. Following mechanisms are involved in the heat transport: heat spreading by baseplate, convective heat transfer between baseplate and liquid, heat transported with the liquid, convective heat transfer between liquid and radiator, heat spreading in the radiator and convective heat transfer between radiator and air.

Based on a system analysis on the simple fluid cooling circuit shown in figure 1, it can be shown that the LED junction temperature is given by [10]:

$$T_j = \left(R_{j-w} + \frac{1}{UA} + \frac{1}{2 \cdot \dot{m}_a \cdot c_{p.a}} \right) \cdot P_c + T_{a.c} \qquad (1)$$

Consider the three terms in the bracket; the first term is the thermal resistance between the LED junction and the temperature of the liquid inside the cold plate (for sketch of material layers and temperature points in the thermal resistance network see figure 2). The second term is the thermal resistance for the radiator used in the cooling circuit, and the third term is related to the amount of air passing through the radiator. Typical values for the three terms are 1...2°C/W, 0.04°C/W (120mm x 120mm radiator) and 0.02°C/W (120mm fan), which shows that the major bottleneck in reducing the junction temperature is the junction-to-water resistance.

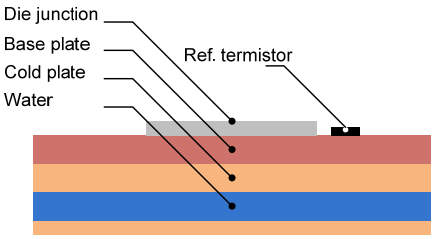

Figure 2: *Material layers in the thermal resistance network of Luminus CBT90 diode and cold plate.*

The junction-to-water resistance represents the sum of the thermal resistance in the LED component ($R_{j\text{-}b}$), Heat sink compound ($R_{b\text{-}hs}$) and cold plate ($R_{hs\text{-}w}$):

$$R_{j-w} = R_{j-b} + R_{b-hs} + R_{hs-w} \qquad (2)$$

where typical values are 0.80K/W for $R_{j\text{-}b}$, 0.12K/W for $R_{b\text{-}hs}$ (this corresponds to app 50micron thick layer of heat sink compound Dow Corning 340) and 0…1K/W for $R_{hs\text{-}w}$. The thermal resistance of the cold plate is given by the conductive heat transfer in the cold plate itself and the convective heat transfer between the cold plate and the fluid circulating through. The convective heat transfer is usually the one which causes the dominating resistance in the cold plate. If the resistance caused by the convective heat transfer has to be minimized, the surface area or the convective heat transfer coefficient must be maximized.

DESIGN OF MINIATURE COLD PLATES

The aim of this paper is to design a cold plate for a high power LED. In this case the Luminus CBT90 LED is chosen as an example of a proper High Power LED, which is relevant for future products in the light industry. The Luminus CBT90 LED has an emitting area of 9mm^2, in which 70W is converted to light and heat. The heat accounts for the major part (up to 95%), and must be considered as waste, which has

to be removed to prevent damage of the LED. The overall dimensions and thermal characteristics of the CBT90 LED relevant for this research are shown in table 1.

Table 1: *Dimensions and thermal characteristics of red, green and blue Luminus CBT90 diode.*

	Red	Green	Blue
LED area (mm^2)	9	9	9
Base area (mm)	28 x 27	28 x 27	28 x 27
Power (W)	40,5	71,6	64,8
$R_{j\text{-}hs}$ (K/W)	0,92	0,92	0,92
$R_{j\text{-}ref}$ (K/W)	0,83	0,83	0,83
$R_{ref\text{-}hs}$ (K/W)	0,09	0,09	0,09
$T_{j\ max}$ (K)	393	423	423
$T_{ref\ max}$(K)	360	364	370

The cold plates which are analysed in this paper must fit the base plate of the selected LED, which has the size of 28mm x 27mm. Due to this the base area of the cold plate is limited to 30mm x 30mm and a height of 10mm, this is in order make it realistic in size for use in moving head lamps. The cold plate design is furthermore restricted of four mounting holes, which purpose is to fasten the diode to the cold plate inside the lamp (the diode is shown in figure 3).

Figure 3: *Red Luminus CBT90 LED diode.*

For further investigation 6 different designs are analyzed through experiments, where a reference temperature is monitored on the LED.

Information on the different cold plate dimensions and surface area exposed to the cooling fluid is given in table 2:

Table 2: *Cold plate dimensions.* (*) *config 4 utilizes a channel with 5/16" - 18 UNC thread. The tapping drill is 6.55mm and the maximum diameter of the thread is 7.938mm.*

Configuration [-]	L [mm]	D_H [mm]	N [-]	A_s [mm^2]	A_c [mm^2]
1	30	4	1	377	12.6
2	71	5	1	1122	19.6
3	25	7	1	550	38,5
4(*)	25	6.55	1	873	33,7
5	25	5	2	785	19,6
6	18	2.86	6	1493	10

The channel design of the 6 configurations are given in figure 4.

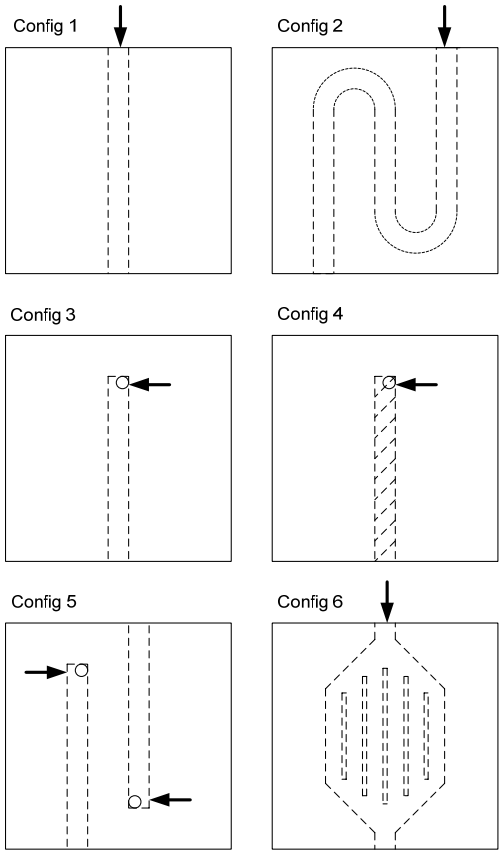

Figure 4: *Cold plate designs. The arrow indicates the fluid inlet to the cold plate. The cold plates given in configuration 3-5 utilize tangential inlet to the cooling channel.*

Analytical Methods

The junction-to-water resistance for the combined diode and cold plate can be calculated as:

$$R_{j-w} = \frac{1}{h \cdot A_s} + R_{j-hs} \tag{3}$$

Where R_{j-hs} is given for the diode in Table 1. The convective heat transfer coefficient is given by:

$$h = \frac{Nu \cdot k}{D} \tag{4}$$

For this calculation the selection of a appropriate Nusselt number relation is critical and dependent flow and geometry. And hence the Nusselt number is depends on dimensions of the geometry, physical properties of the fluid, and fluid velocity, it is not possible to select a single Nusselt number correlation, which covers all 6 geometrie.

In configuration 1 the flow field is assumed to develop in the cold plate (the cooling fluid is flowing in a tube with a slightly larger diameter and an entrance with a sharp edge exist at the inlet to the cold plate). For Re above 200, the flow will never be thermally fully developed in the cold plate ($L_{t.laminar} = 0.05 \cdot Re \cdot Pr \cdot D$ or $L_{t.turbulent} \approx 10 \cdot D$) [1].

For laminar flow (Re≤2300) the Nusselt number is given by [11]:

$$Nu_D = 3.66 + \frac{0.065 \cdot (D/L) \cdot Re \cdot Pr}{1 + 0.04 \cdot \left((D/L) \cdot Re \cdot Pr\right)^{2/3}} \quad (5)$$

For fully developed turbulent flow the Nusselt number is given by Gnielinski's formula (valid for 0,5 < Pr < 2000 and 3000 < Re < 10^6) [11]:

$$Nu_D = \frac{(f/8)(Re_D - 1000)Pr}{1 + 12.7(f/8)^{1/2}(Pr^{2/3} - 1)} \quad (6)$$

The friction factor f is found in the Moody chart to 0.065-0.059 at Re ≈ 2300-6000 and relative roughness ≈ 0.025 (in literature appropriate expressions for the friction factor is given by C. F. Colebrook or S. E. Haaland). In the case of turbulent flows the heat transfer coefficient is corrected by h/h_∞ to take inlet effects into account [11]. The correction factor (h/h_∞) is found in figure 3 (for x/D=6 it is 1.26).

Configuration 2 is calculated according to the same procedure as configuration 1 – but with the h/h_∞ correction corresponding to a 180° bend (correction factor 1.26) [11]. The larger surface area in configuration 2 reduces the thermal resistance and hence the junction temperature of the diode.

Configuration 3, 4 and 5 utilizes swirling flows, which has a tendency to squeeze the boundary layer and thereby enhance the local heat transfer coefficient. Research on heat transfer enhancement by swirling flows has been carried out by several authors [12] [13] [14]. The effect of this enhanced heat transfer is a lower thermal resistance due to convection and hence a lower junction temperature of the diode. Based on an experimental study Guo and Dhir [12] present the following equation for the enhancement of the Nusselt number (valid for 2,3 < P r <6,3 in range $1.2 \cdot 10^4$ < Re < $6.0 \cdot 10^4$):

$$\frac{Nu_s^*}{Nu_{fd}^*} = 1 + 0{,}48e^{-0{,}4(z_j/D)} + 2{,}3\left(\frac{M_t}{M_T}\right)^{0{,}68} e^{-0{,}22(z_j/D)^{0{,}56}Pr^{0{,}25}} \quad (7)$$

This equation correlates 90% of the experimental data within ±10%. This equation is used for both laminar and turbulent flow regimes in despite of the valid Re region is well above what is expected for this study.

In the last configuration (config 6) the channel dimensions are smaller and the surface area is increased compared to configuration 1. For laminar flow the Nusselt number is determined by the equation valid for the entrance region (developing) for flows between parallel plates (valid for Re≤2800) [1]:

$$Nu_D = 7.54 + \frac{0.03 \cdot (D_H/L) \cdot Re \cdot Pr}{1 + 0.016 \cdot \left((D_H/L) \cdot Re \cdot Pr\right)^{2/3}} \quad (8)$$

For turbulent flow the Nusselt number is determined by Gnielinski's formula given in equation 6. Similar to configuration 1 and 2 the entrance effect is taken into account. Here the open end correction factor is applied (for x/D=9 it is 1.57).

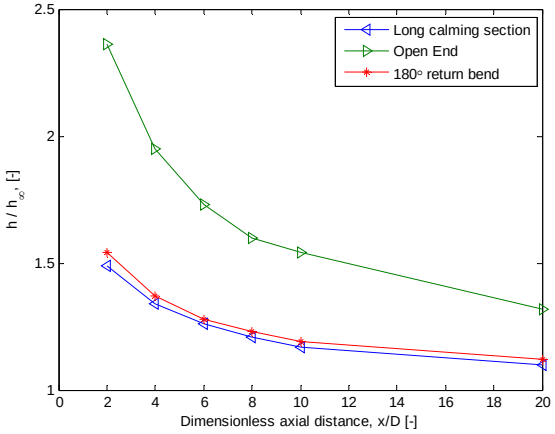

Figure 5: *Effect of entrance configuration on average heat transfer coefficient for turbulent flow in pipes, based on A.F. Mills* **[11].**

Experimental Methods

Prototypes of the different cold plates are manufactured copper and tested with a Blue Luminus Phlatlight CBT-90 LED. The cold plate and diode is assembled with Dow Corning 340 heat sink compound as interface material. 8mm plastic tubes are glued on the heat sink and connected to the cooling circuit according to the diagram sketched in figure 6. Distilled water is used as cooling fluid.

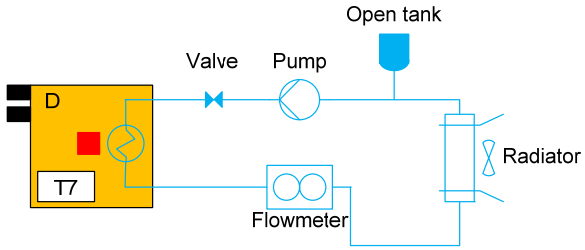

Figure 6: *Schematic view of water cooling circuit.*

The water is circulated continuously through the system by a 12V Biltema pentry pump, with a maximum capacity 6.6l/min at 2m lifting height (no further information is available). The flow is regulated by powering up/down the pump and eventually by adjusting the pressure loss in the circuit by a valve downstream the pump. The water flow is measured by an in-line flow sensor (RS257-149), with a flow range of 0.25-6.5l//min (± 1% FSD linearity). The Pressure difference between inlet and outlet of the cold plate is measured with a Huba type 692 differential pressure transducer . The diode is driven by a Delta Elektronika SM70-22 power supply. The cold plate mounted with the LED is placed inside a test cube with a thermal resistance of 9K/W. By measuring the air temperature outside and inside the test cube it is possible to estimate the heat generated as radiation from the die itself. For computerized data acquisition a laptop

computer equipped with LabVIEW and National Instrument data acquisition hardware is used (data acquisition components are given in table 3).

Table 3: *Hardware used for testing cold plate performance.*

Equipment	Description	Measurand
NI-9172	Compact Daq	-
NI-9211	Thermocouple module	Temperature (T1-T3)
NI-9211	Thermocouple module	Temperature (T4-T6)
NI-9401	Digital module	Flow (FM)
NI-9219	Multi purpose module	Resistance (R)
	Multimeter	Voltage (U)
	Multimeter	Current (I)

Temperatures in the experimental setup were measured according to the figure 7. All data are monitored for minimum 30minutes to ensure steady state, after which 300 samples for each measurand are acquired over a period of 12.5minutes.

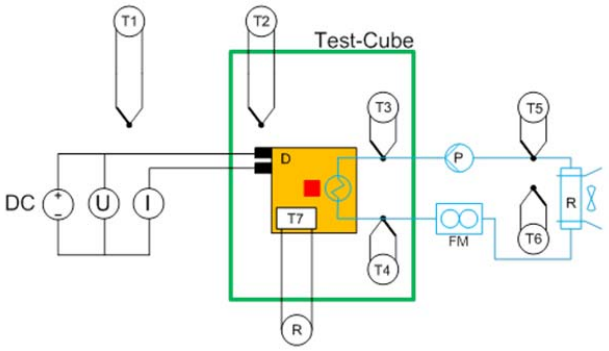

Figure 7: *Experimental setup used in cold plate experiments.*

The differential pressure across the cold plate and the pumping power for the different configurations were measured in addition to the thermal measurements on cold plate performance. This information is used for final evaluation of best performing cold plate design.

Data reduction

For the analytical data, the reported temperature ($\Delta T_{Ref\text{-}w}$) in the results and discussion section is the temperature difference between cooling fluid and LED reference thermistor (T7 on figure 7), hence the LED junction temperature can only be measured indirectly by the LED reference thermistor added a calculated reference-to-junction temperature. The temperature difference between cooling fluid and the thermistor is given by:

$$T_{Ref} = R_{Ref-w} \cdot P_c + T_w \tag{9}$$

Where P_c is the input power to the LED and the thermal resistance $R_{T\text{-}hs}$ is given by:

$$R_{Ref-w} = \frac{1}{h \cdot A} + R_{Ref-hs} \tag{10}$$

The analytically determined heat transfer coefficient, h, is predicted by an appropriate Nusselt number correlation matching flow and channel layout of the cold plate.

For the experimental data the reported temperature ($\Delta T_{Ref\text{-}w}$) is the difference between the thermistor temperature and the temperature of the water in the cold plate.

RESULTS AND DISCUSSION

Analytical results

The thermistor temperature on the CBT90 LED is predicted for 6 cold plate designs, which are presented in previous sections of this paper. In figure 8 the temperature difference between the thermistor and cooling fluid is presented for volume flows between 5ml/s and 20ml/s through the cold plate.

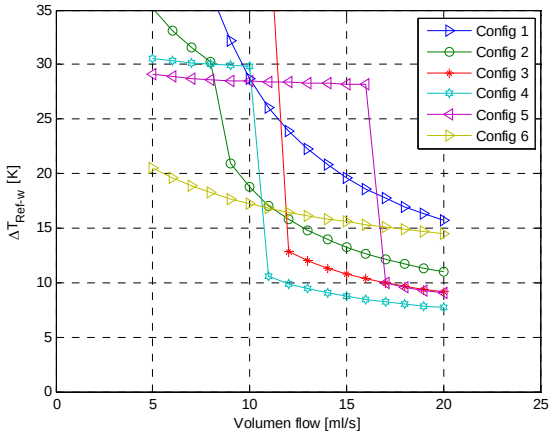

Figure 8: *Calculated temperature difference between the diode reference thermistor and average water temperature.*

For configuration 2 to 5 the temperature difference seems to be almost discontinuous at flows somewhere in the region of 8ml/s to 16ml/s. This is the effect of changing the Nusselt number correlation from laminar to turbulent flows, when the Reynolds number exceeds 2300. For configuration 1 this happens for a volume flow of 6.4ml/s. As a result of this the nature of the flow in configuration 1 is more or less turbulent in the entire investigated flow range. For configuration 6, the opposite happens as the transition to turbulent flows occurs at 27.5ml/s. The flow rate where the theoretical transition from laminar to turbulent flow occurs are given in table 4 for the different cold plate configurations.

Table 4: *Flow rates where theoretical transition from laminar to turbulent flow occurs (Re=2300).*

Configuration [-]	1	2	3	4	5	6
Flow [ml/s]	6.4	8.0	11.2	10.5	16.0	27.5
Re	2300	2300	2300	2300	2300	2300

As expected the cooling performance of configuration 1 is poor, this is due to a low heat transfer coefficient in combination with the lowest surface area. Configuration 2 perform slightly better primarily due to a larger surface area of the cooling channel, but the transition from laminar to

turbulent flow occurs at higher flow rates due to a smaller cross sectional area. The configurations 3-5 all have relatively poor cooling capacities at lower flow rates compared to configuration 6. This can be explained by low heat transfer coefficients in the laminar flow regime and the fact, that configuration 6 has 2-3 times the surface area of configuration 3-5. For higher flow rates configuration 3-5 have the best cooling capacities. This is due to a strong swirling flow, which squeezes the boundary layer towards the outer wall, and thereby maximizes the heat transfer. Configuration 6 seems to perform well at lower flow rates, where it has the best cooling capacity, while it has lower cooling capacity at higher flow rates compared to the other configurations. This is due a late transition from laminar to turbulent flow, which happens outside the considered flow range.

Experimental Results

All 6 configurations are tested during experiments in the laboratory, and the results are presented in figure 9. The test did not show any discontinuity in temperature differences as shown in the analytical calculations. Most surprising is that the straight channel in configuration 1 deviates significantly from the predicted values at low flow rates. An explanation could be transition to turbulent flow at a low Reynolds number due to disturbance from flow meter and thermo couples near the inlet to the cold plate. The same tendency is present for the experimental date for the remaining 5 configurations, where the measured temperature difference between thermistor and cooling fluid is quite low in comparison with the predicted temperature difference.

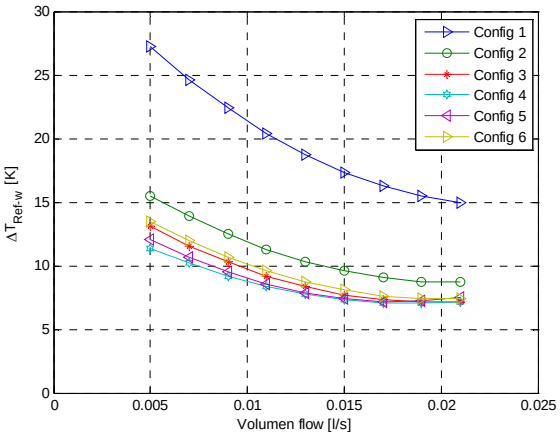

Figure 9: *Measured temperature difference between the diode reference thermistor and average water temperature in the cold plate.*

Based on the temperature measurements versus flow rate, it is clear that configuration 1 is not recommendable, while it is difficult to distinguish between the remaining 5 designs. The final choice of cold plate to the LED based on the designs tested in this study may include considerations about pressure loss in the cooling system and production cost. Pressure measurements versus flow rates are presented in figure 10. As expected there are high pressure losses in the cold plates utilizing swirling flows, this is due to a small diameter in the tangential inlet tube.

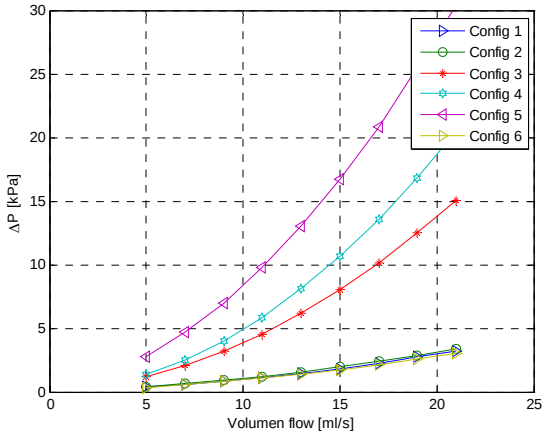

Figure 10: *Pressure difference across the cold plate vs flow rates for the 6 cold plate configurations.*

Combining the information in figure 9 and figure 10 gives a more realistic picture for evaluation of cold plate performance versus pressure loss in the cold plate (figure 11).

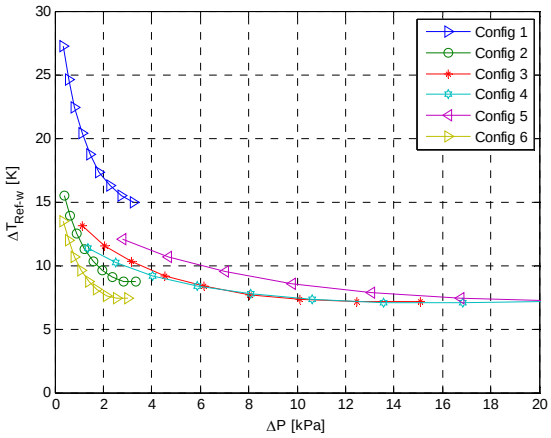

Figure 11: *Measured temperature difference between the diode reference thermistor and average water temperature in the cold plate versus pressure difference across the cold plate.*

It turns out that configuration 6 performs best followed by configuration 2 when looking at both cooling capability and pressure loss in the cold plate, but looking at the channel design they are also the most difficult to fabricate. A good alternative is configuration 3 utilizing swirling flows. If a higher pressure loss can be accepted.

CONCLUSION

This paper deals with cooling of a blue Luminus Phlatlight CBT90 high power LED. 6 different layouts of cooling channels are studied both analytically and experimentally at different flow rates. The measured and calculated temperatures at a reference point on the LED are compared.

The analytically calculated reference temperatures show a discontinuity in temperature curves versus flow rates. The experiments did not show this discontinuity. The experiments

show furthermore better cooling performance than predicted. The discontinuity in the temperature curves is expected to be a result of poor accuracy in Nusselt number relations, when the flow is in proximity of transition from laminar to turbulent. The poor agreement in predicted cooling performance at lower flow rates is properly due to disturbances from thermo couples mounted in the tube upstream the inlet to the cold plate, which causes the flow to be turbulent even at lower flow rates.

References

[1] Yunus A. Cengel, *Heat transfer - a practical approach*. New York: McGraw - Hill, 2003.

[2] Ugo Lafont, Henk van Zeijl, and Sybrand van der Zwaag, "Increasing the reliability of solid state lighting systems via self-healing approaches: A review," *Microelectronics Reliability*, vol. 52, pp. 71-89, 2012.

[3] Jason Posselt, "Evolutionary LED Packaging for Increased Flux Density," *LED Professional review (LpR)*, pp. 24-27, May/June 2008.

[4] Mick Wilcox, "Thermal Management - An In-Depth Look at Active Cooling Thermal Management: Synthetic Jet Technology," *LED professional Review (LpR)*, pp. 36-40, may/june 2008.

[5] Jingsong Li et al., "Analysis of Thermal Field on Integrated LED Light Source Based on COMSOL Multi-physics Finite Element Simulation," *Physics Procedia*, vol. 22, pp. 150-156, 2011.

[6] Sheng Liu, Jianghui Yang, Zhiyin Gan, and Xiaobing Luo, "Structural optimization of microjet based cooling system for high power LEDs," *International Journal of Thermal Sciences*, vol. 47, pp. 1086-1095, 2008.

[7] Jian-hua Xiang, Chun-liang Zhang, Fan Jiang, Xiao-chu Liu, and Yong Tang, "Fabrication and testing of phase change heat sink for high power LED," *Transactions of Nonferrous Metals Society of China*, vol. 21, pp. 2066-2071, 2011.

[8] Seung-Hwan Yu, Kwan-Soo Lee, and Se-Jin Yook, "Optimum design of a radial heat sink under natural convection," *International Journal of Heat and Mass Transfer*, vol. 54, pp. 2499-2505, 2011.

[9] Adam Christensen and Samuel Graham, "Thermal effects in packaging high power light emitting diode arrays," *Applied Thermal engineering*, vol. 29, pp. 364-371, 2009.

[10] Henrik Sørensen and Søren Nørgaard Bertel, "Design of Miniature Liquid Cooler for LED," in *Proceedings of the ASME/JSME 2011 8th Thermal Engineering Joint Conference*, Honolulu, 2011.

[11] Anthony F. Mills, *Heat and Mass Transfer*.: IRWIN, 1995.

[12] Z. Guo and V. K. Dhir, "Single- and two-phase heat transfer in tangential injection-induced swirl flow," *International Journal of Heat and fluid flow*, vol. 10, no. 3, pp. 203-210, september 1989.

[13] S. Martemianov and V. L. Okulov, "On heat transfer enhancement in swirl pipe flows," *International Journal of Heat and Mass Transfer*, vol. 47, pp. 2379-2393, 2004.

[14] D. Lelea, "effects of inlet geometry on heat transfer and fluid flow of tangential micro-heat sink," *Internation Journal of Het and Mass Transfer*, vol. 53, pp. 3562-3569, 2010.